Reducing friction between metal and thermo-mechanical pulp using alkyl ketene dimers and magnesium stearate

Tribology International 192 (2024) 109280

Contents lists available at ScienceDirect

Tribology International

journal homepage: www.elsevier.com/locate/triboint

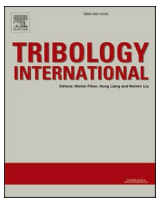

Reducing friction between metal and thermo-mechanical pulp using alkyl ketene dimers and magnesium stearate

Seyedehsan Hosseini [a], Roujin Ghaffari [a,b], Anette Larsson [a,b,c], Gunnar Westman [b,c,d], Anna Ström [a,c,*]

[a] Applied Chemistry, Chemistry and Chemical Engineering, Chalmers University of Technology, Gothenburg, Sweden
[b] Wallenberg Wood Science, Chemistry and Chemical Engineering, Chalmers University of Technology, Gothenburg, Sweden
[c] FibRe, Chemistry and Chemical Engineering, Chalmers University of Technology, Gothenburg, Sweden
[d] Organic Chemistry, Chemistry and Chemical Engineering, Chalmers University of Technology, Gothenburg, Sweden

ARTICLE INFO

Keywords:
Three balls on plate
3BOP
Roughness
Profilometer

ABSTRACT

The friction between natural fibers and metal affects tool life, wear and tear and surface defects of extrudates. The ability of alkyl ketene dimer (AKD) and magnesium stearate (MgSt) to reduce coefficient of friction (COF) between thermomechanical pulp (TMP) and metal were determined at temperatures of 30, 100, and 180 °C and additive concentrations from 0.5 to 5 wt%. The AKD and MgSt were added to TMP sheets through spraying, followed by drying. ATR-FTIR and IR microscopy confirmed the presence of AKD and MgSt on the TMP. AKD addition at 2 wt%, consistently reduced the COF of TMP and metal, whereas MgSt reduced COF at 100 and 180 °C, only. No further reduction in COF was observed at 5 wt% of AKD or MgSt.

1. Introduction

The growing concerns over global warming and declining fossil fuel resources have created a demand for alternative resources to synthetic polymers in the production of plastic-like materials [1,2]. Wood has a rich history of utilization by humans spanning several millennia. Wood possesses an array of desirable properties, including a high degree of stiffness and strength relative to its weight [3]. The conversion of timber into various products generates wood powder and sawdust [4]. Wood powder and saw dust are used as low cost and renewable fillers in wood plastic composites (WPC). WPCs have application as decking, as materials within the automotive industry or as building material where the low density of the natural filler is an advantage [4] and where the use of wood fibres, instead of saw dust or wood powder, have the additional advantage of providing mechanical strength. If the materials are subjected to sliding motion, they must also accommodate properties such as low coefficient of friction (COF) and wear rate, which can be obtained through absorption of oil (up to 2.5 wt%) [5]. Refining wood chips yields a fibre referred to as thermomechanical pulp (TMP). TMP has advantages over fibres from sulphite or kraft pulp, as it is cheaper, obtained without use of chemicals and with a high yield [4]. Common challenge for WPCs, produced with fibres such as TMP, is their poor flow behaviour during thermal processing [6–8], generating flow instabilities and surface defects such as uneven or rough extrudate surfaces [6]. Surface defects are reduced at high extrusion rates and high shear rates [6], which is linked to increased wall slip and slip velocity between extruder or die and the WPC [6,9]. Similar findings are known from the field of metal extrusion, where addition of lubricants to nickel improves the appearance of the nickel extrudate surface [10]. We have shown that the addition of alkyl ketene dimer (AKD) to TMP-polypropylene composites reduces surface defects of the extrudate at a TMP loading of 50 wt% [11]. The reduction of surface defects in presence of long chain AKDs could be related to the observed reduction in melt viscosity of the WPC, however, the reduction was small. Therefore, we want to investigate whether the addition of AKD and magnesium stearate (MgSt) to TMP surface reduces the friction between TMP and metal, at temperatures relevant for extrusion. Both additives (AKD and MgSt) are commonly available and do not require added steps of chemical modification. AKD is a sizing agent used in the paper industry [12,13]. MgSt is employed as lubricant within the pharmaceutical industry, notably for its anti-adherent and lubricant properties within production of solid formulations [14,15].

While wear and tear studies of composite materials using natural fibres exist [16–18], and wood and metal [19–22] to the best of our

* Corresponding author at: Applied Chemistry, Chemistry and Chemical Engineering, Chalmers University of Technology, Gothenburg, Sweden.
E-mail address: anna.strom@chalmers.se (A. Ström).

https://doi.org/10.1016/j.triboint.2024.109280
Received 23 October 2023; Received in revised form 22 December 2023; Accepted 8 January 2024
Available online 10 January 2024

Table 1
Samples, type of additive, theoretical weight percentage of added additive as well as measured mass difference of TMP sheet prior and post lubricant addition and drying. Three sheets were measured and number within parenthesis is standard deviation (SD).

Sample	Additive	Theoretical weight of additive / %	Mass difference, in % between dry TMP sheet prior and post addition of additives
TMP	None	0	0
TMP AKD0.5	AKD	0.5	0.7 (0.0)
TMP AKD2	AKD	2.0	1.7 (0.1)
TMP AKD5	AKD	5.0	5.4 (0.9)
TMP MgSt0.5	MgSt	0.5	0.8 (0.0)
TMP MgSt2	MgSt	2.0	2.5 (0.0)
TMP MgSt5	MgSt	5.0	5 (0.6)

knowledge, few studies have focused on friction between TMP and metals at temperatures relevant for extrusion of WPCs. Reduction in moisture of wood leads generally to a reduction in COF between wood and metal, whereas addition of water increases the COF [19] and non-dried wood fiber increases surface defects of WPCs through bubble formation [9]. COF between wood and metal varies as a function of temperature but exact temperatures vary between studies. Murase showed that the COF between wood and metal is reduced at temperatures above 120 °C [20], whereas Engberg and co-workers showed an increase in COF between wood and metal at 160 °C [21]. Friction of wood at high temperatures has also been studied within the field of rotary friction welding of wood [22]. Control of COF between TMP and metal can contribute to reduced surface defects of WPC extrudates, extend tool life [23], and facilitate the use of TMP in material subjected to sliding motions [6].

Our aim was to reduce COF between metal and TMP sheets through the addition of AKD and MgSt. The ability of the AKD and MgSt to reduce COF between metal and TMP was investigated at different temperatures (30, 100 and 180 °C). AKD and MgSt were dissolved in a blend of ethanol / dieter and sprayed onto hand-made sheets of TMP. The influence of AKD and MgSt on the roughness and visual impression of TMP sheets were examined using optical profilometry and scanning electron microscopy (SEM). COF was obtained between TMP sheets and metal balls using three balls on plate. The results show that both AKD and MgSt reduce COF between metal and TMP at temperatures > 100 °C, while not impacting surface roughness of the TMP sheets.

2. Material and methods

The TMP was obtained from Stora Enso Hyltebruk, Sweden and sourced from Norway spruce (Picea abies). The TMP had a mean fiber length, width, and fines content of 3.2 mm, 35 μm, and 33%, respectively [24]. As per the literature, TMP comprises 50 wt% polysaccharides and approximately 30–35 wt% lignin [25]. The AKD wax, AQUAPEL 291-EU, was provided by Solenis Sweden AB and had a C18 alkyl chain length. MgSt, Extra Pure, SLR, was provided by Fisher Scientific.

2.1. Paper sheets for friction tests

Sheets were formed using TAPPI/ANSI T 205 sp-18 standard [26]. TMP fibers, equivalent to three sheets (3.6 g), were suspended in 1.2 l deionized water using a standard pulp disintegrator at 2900 revolutions per minute for 60,000 rotations (Lorentzen & Wettre, Sweden). Sheets were formed, blotters were placed on the wet sheets, and excess water was removed using a couch roll. The stack of sheets was pressed at 345 kPa for five minutes, blotters were changed, and the test sheets were pressed again pressed for two minutes at 345 kPa. The sheets were air-dried for ten days.

2.2. Disposition of additives on TMP sheets

Different proportions of AKD and MgSt were dissolved in a fixed volume (50 mL) of ethanol and diethyl ether (40:60 wt% ethanol and diethyl ether, respectively). The volume was fixed to expose the fibers to an equal amount of solvent, and the concentrations of AKD and MgSt in the solvent mixture were adjusted to yield 0.5, 2 and 5 (wt%) of additives relative to dry mass of the TMP sheet. The solutions were sprayed onto the TMP sheets and dried in a fume hood (at room temperature) for 24 h. TMP sheets without AKD or MgSt were treated similarly, that is, the sheets were sprayed with the same amount of ethanol-diethyl ether, followed by drying in a fume-hood for 24 h. Table 1 outlines the samples used throughout the study, and their theoretical composition.

2.3. Attenuated total reflectance Fourier transform infrared spectroscopy (ATR-FTIR)

ATR-FTIR was performed using a Perkin Elmer Frontier FT-IR Spectrometer (Waltham, MA, USA), equipped with a diamond Gladi-ATR attenuated total reflectance (ATR) attachment from Pike Technologies. The samples, which were measured in triplicates, were placed directly on the ATR-crystal without further preparation. The spectra were recorded between 4000 and 400 cm^{-1}, based on 32 scans with a resolution of 4 cm^{-1} at intervals of 2 cm^{-1}.

2.4. IR microscopy

To investigate the uniformity of AKD and MgSt on the surface of the samples, a Hyperion 3000 microscope coupled to a Vertex 70 v FT-IR spectrometer (Bruker, Ettlingen, Germany) was used. A 49-point (7 × 7) grid was defined within a rectangular area measuring 220 μm by 160 μm, ensuring coverage of the entire region of interest. To record the IR spectra at each point of the grid, a 15x ATR objective and 64 × 64 MCT FPA detector were used between 3900 and 900 cm^{-1} at 4 cm^{-1} resolution under N_2 purge. To obtain a good signal-to-noise ratio, 16 scans per spectra were recorded and averaged.

The recorded spectra were first baseline corrected using OPUS 7.5. software. Subsequently a MATLAB code was used to integrate the area under the spectra between 2790 to 3000 cm^{-1}. Based on the 49-point grid, an image was constructed using the integrated areas to visualize the distribution of MgSt and AKD on the sample surface.

2.5. Optical profilometry

An optical profilometer (Sensofar S neox, Spain) was used to measure the surface roughness of TMP sheets of dimensions 3 cm × 3 cm. A 3D surface was reconstructed by confocal imaging using a 20x EPI objective. Open-source software Gwyddion was used to calculate a roughness based on penetration and geometry of the rotating balls employed for friction determination. The penetration height was calculated from measuring the height of the TMP sheet at a normal force of 0 (H_{F0}) and normal force of 1 N (H_F), as determined using the rheometer. The difference between the heights ($H_F - H_{F0}$) defined the penetration depth.

2.6. Scanning electron microscopy

The surface of TMP sheets were imaged using a Leo Ultra 55 FEG SEM, Germany, and the images were taken with a secondary electron

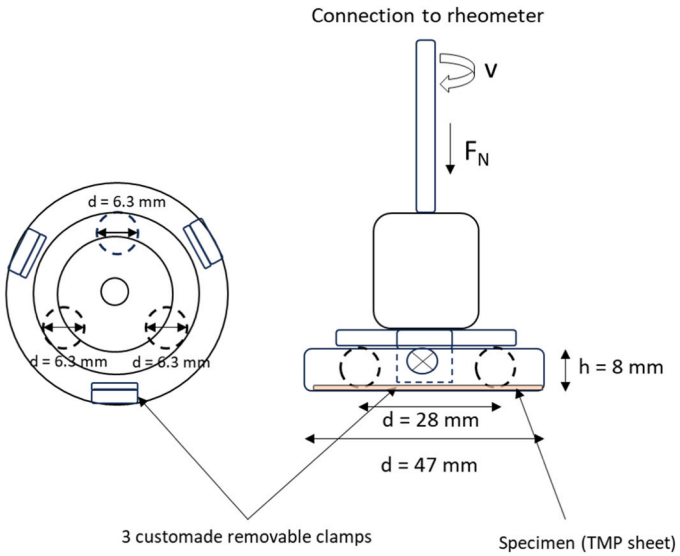

Fig. 1. Schematic drawing of the three balls (d = 6.3 mm) on plate geometry (purchased from TA Instruments), with a custom made device of three clamps fixating the specimen (TMP and TMP AKD, TMP MgSt sheet) during measurement.

detector at 3.0 kV. The samples were sputter coated with gold before measurement.

2.7. Differential scanning calorimetry

The thermal transitions and the crystallinity of the materials were assessed using a Mettler Toledo DSC2 calorimeter, USA, equipped with a HSS7 sensor (USA) and a TC-125MT intercooler (USA). The endotherms were recorded while the temperature was increased from 30 °C to 250 °C at a scan rate of 10 °C/min with a nitrogen flow of 50 mL/min.

2.8. Friction measurements

A DHR-3 rheometer from TA instrument (USA), equipped with a three-balls-on-plate (3BOP) was employed to investigate the effect of AKD and MgSt on the friction between metal and TMP sheets. The geometry consists of three stainless steel spheres with a diameter of 6.3 mm. The paper sheets were affixed to the lower plate utilizing a combination of double-sided tape and customized clamps (Fig. 1), ensuring secure immobilization of the sheets during the experimental procedure. The experiments were conducted at 30, 100 and 180 °C. The temperature was kept constant using an environmental test chamber (purchased from TA instruments, USA). The TMP, TMP AKD and TMP MgSt sheets varied in height (from 400 to 600 μm) why zero gap was determined for each sheet and each temperature used. The COF obtained between the samples and metal balls was determined at a constant sliding distance of 50 m, a sliding speed of 100 mm/s, and an axial force of 1 N. The COF is obtained from Eq 2, F_f and F_N are the friction and normal force, respectively.

$$COF = \frac{F_f}{F_N} \quad (1)$$

2.9. Statistical analysis

Statistical analysis was conducted using the Origin data analysis software (OriginLab Corporation, Northampton, MA, USA), employing a one-way analysis of variance (ANOVA) test to assess differences among multiple groups. Significance level was set at $p < 0.05$.

3. Results and discussion

3.1. Addition and quantification of additives to the TMP sheets

The variations in mass between TMP sheets, before and after being sprayed with AKD or MgSt dissolved in ethanol and diethyl ether were used to quantify the residual solvent and additive remaining at the surface or within the TMP sheet (Table 1). The results show that the mass of the TMP sheets increased when sprayed with dissolved additive. We observe that the lower amount of additive (0.5 wt%) had higher

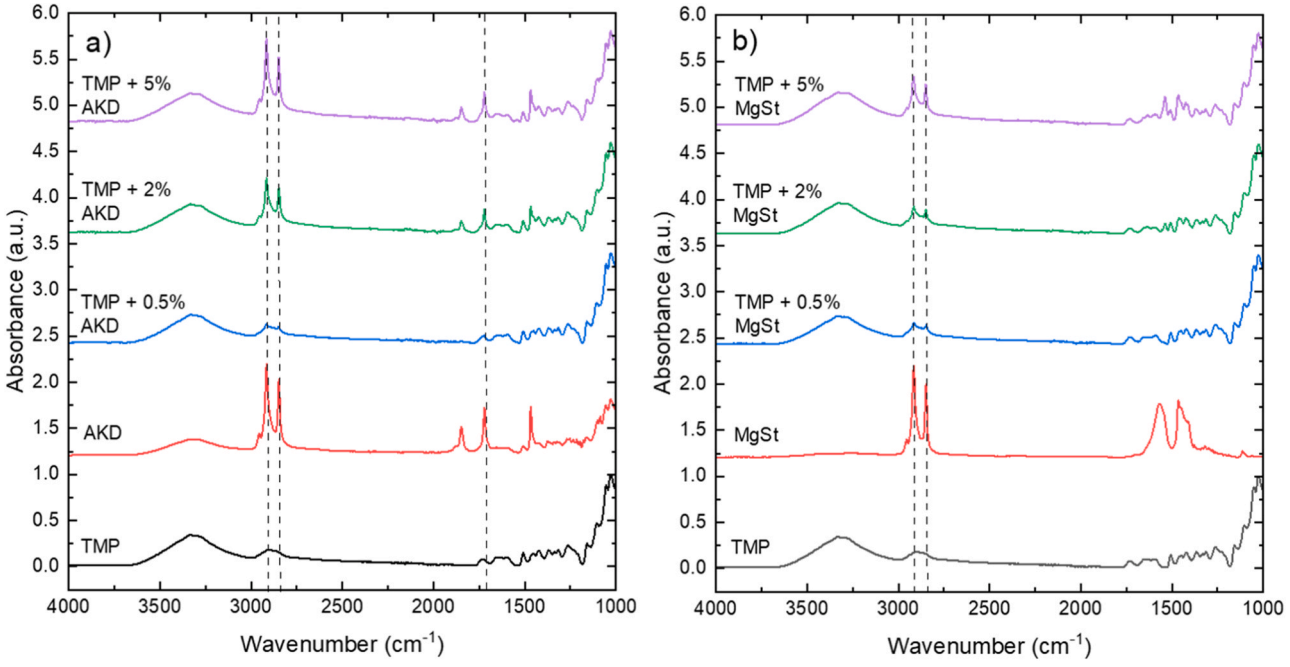

Fig. 2. IR spectra of TMP, additive and TMP with additive at increasing concentration (0.5–2 wt% of a) AKD and b) MgSt. The spectra have been shifted with 1.2 units to each other. Dotted lines are added at wavenumber of 2916, 2845 and 1720 cm^{-1}.

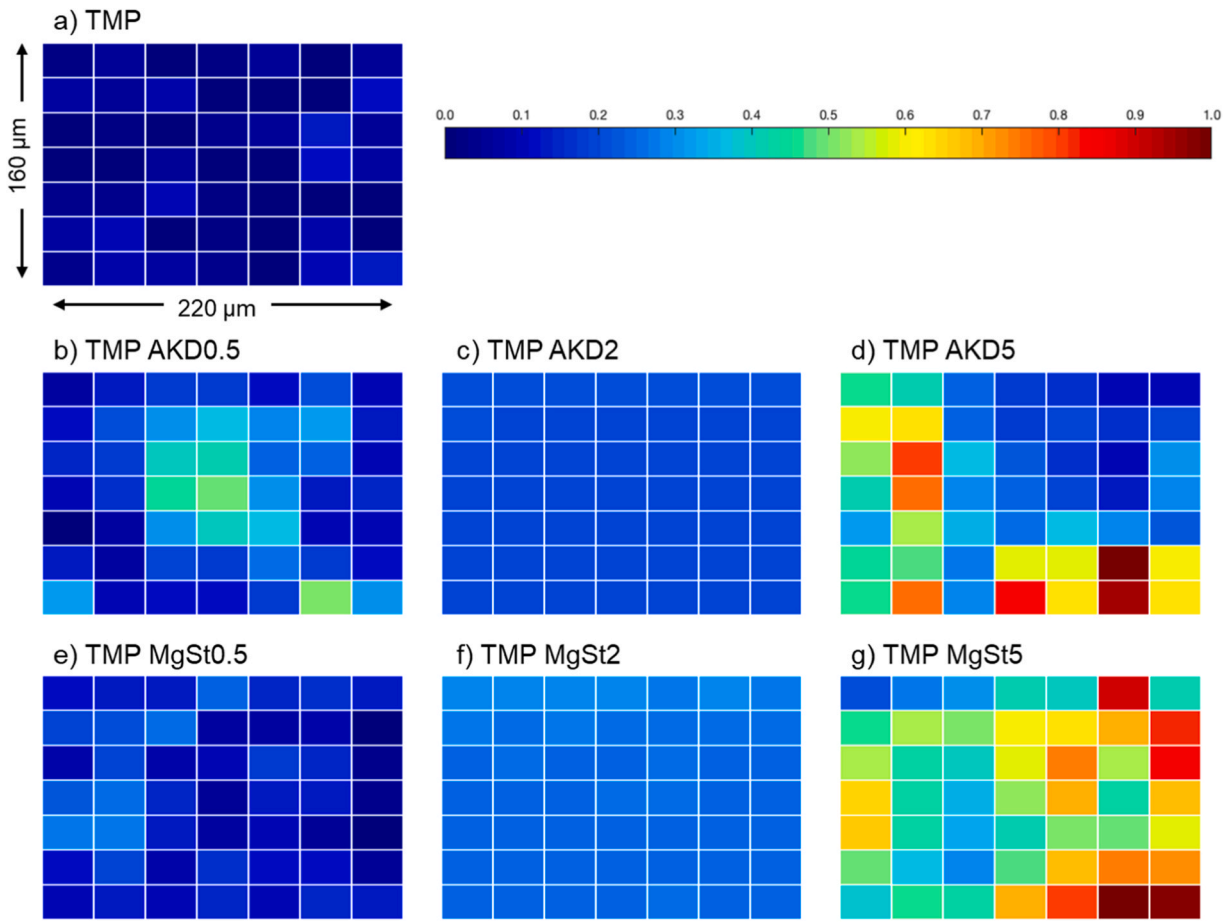

Fig. 3. IR microscopy images of a) TMP sheets (b-d) TMP sheets with added AKD and (e-g) TMP sheets with added MgSt at increasing concentration. Bar graph shows a transition in the peak intensity (2845 and 2916 cm^{-1}) with dark blue depicting low and dark red to brown high transition in peak intensity.

weight increase than expected (0.7% and 0.8%) for AKD and MgSt respectively. The mid-range of 2 wt% was determined to be 1.7 and 2.5 wt% through mass analysis of AKD and MgSt, while the highest amount of 5 wt% is 5.4 and 5 for AKD and MgSt respectively. Fig. 2a depicts the IR spectra of TMP sheets and TMP with increasing amounts of AKD. The intensity of the carbon chain peak within the 2845 and 2916 cm^{-1} range increased with AKD concentration. Furthermore, a new peak corresponding to the carbonyl group emerged in the range of 1720 cm^{-1}. The increased intensity of the peaks corresponding to carbon chain and carbonyl groups, confirms the presence of AKD on the TMP. Fig. 2b shows the IR spectra of TMP and TMP with increasing amounts of added MgSt. Similarly, as for the AKD addition, the intensity of the peak corresponding to carbon chain increased for TMP MgSt samples, which confirms the presence of MgSt on the TMP sheets.

The distribution of the AKD and MgSt over the surface of the TMP sheets is shown in Fig. 3. The color of the bar graph corresponds to the concentration of the additive, where dark blue depicts no or little concentration of additive and dark red to brown depicts highest concentrations. Fig. 3a shows the reference image of TMP surface without any added AKD or MgSt. The image displays mostly dark blue colors, thus at the low-end spectra of added compounds. Figs. 3b and 3e show more light blue colors, and especially 3b, shows lighter blue colors, indication of heterogeneously distributed AKD, as compared to MgSt, which appears more homogeneously distributed. Increasing the concentration to approx. 2 wt% shows a homogeneous light blue color, indicating a more even spread of AKD and MgSt over the TMP surface, followed by red and dark red color at the highest additive concentration of approx. 5 wt%. AKD at approx. 5 wt% appears to spread less evenly than MgSt, at similar concentration. The AKD sample shows large variation in blue (depicting low concentrations of AKD) and red (depicting high concentrations of AKD) displayed in Fig. 3d.

The weight difference, FT-IR and IR microscopy confirm the presence of AKD and MgSt on the TMP sheet close to concentrations of.5, 2 and 5 wt%.

3.2. *TMP roughness independent of additive additions*

The roughness of the TMP sheets sprayed with ethanol and diethyl ether and the TMP sheets sprayed with AKD and MgSt dissolved in ethanol and diethyl ether was determined using optical profilometry. The roughness of the TMP sheet was 25 ± 7 µm. The roughness between the sheets with no and different type of additive (AKD and MgSt) and at different concentrations showed no statistically significant difference (Fig. S1), except the sample of TMP with 0.5 wt% AKD, which had a statistically significantly lower roughness than TMP sprayed with TMP of 5 wt% AKD. The TMP AKD0.5 samples had a roughness of 20 ± 5 µm and TMPAKD5 had a roughness of 35 ± 7 µm, respectively. The statistical significance is only between these two samples and not between the TMP AKD0.5 and control (TMP).

SEM was employed to visually examine the surface morphology of the TMP sheets and assess the impact of additives (Fig. 4). Fig. 4a and b, show the unmodified TMP sheet, revealing the network of TMP fibers at two different magnifications (1000 and 5000X). As expected from the fiber size analysis using Kajaani, the fibers are on the millimeter scale in length, micrometer in width, and polydisperse [24]. The surfaces of the TMP fibers show small pits (appear as holes in the fibre), which are naturally present in softwood, with the function of transporting water from one tracheid to another. Particles of spherical shape are visible in

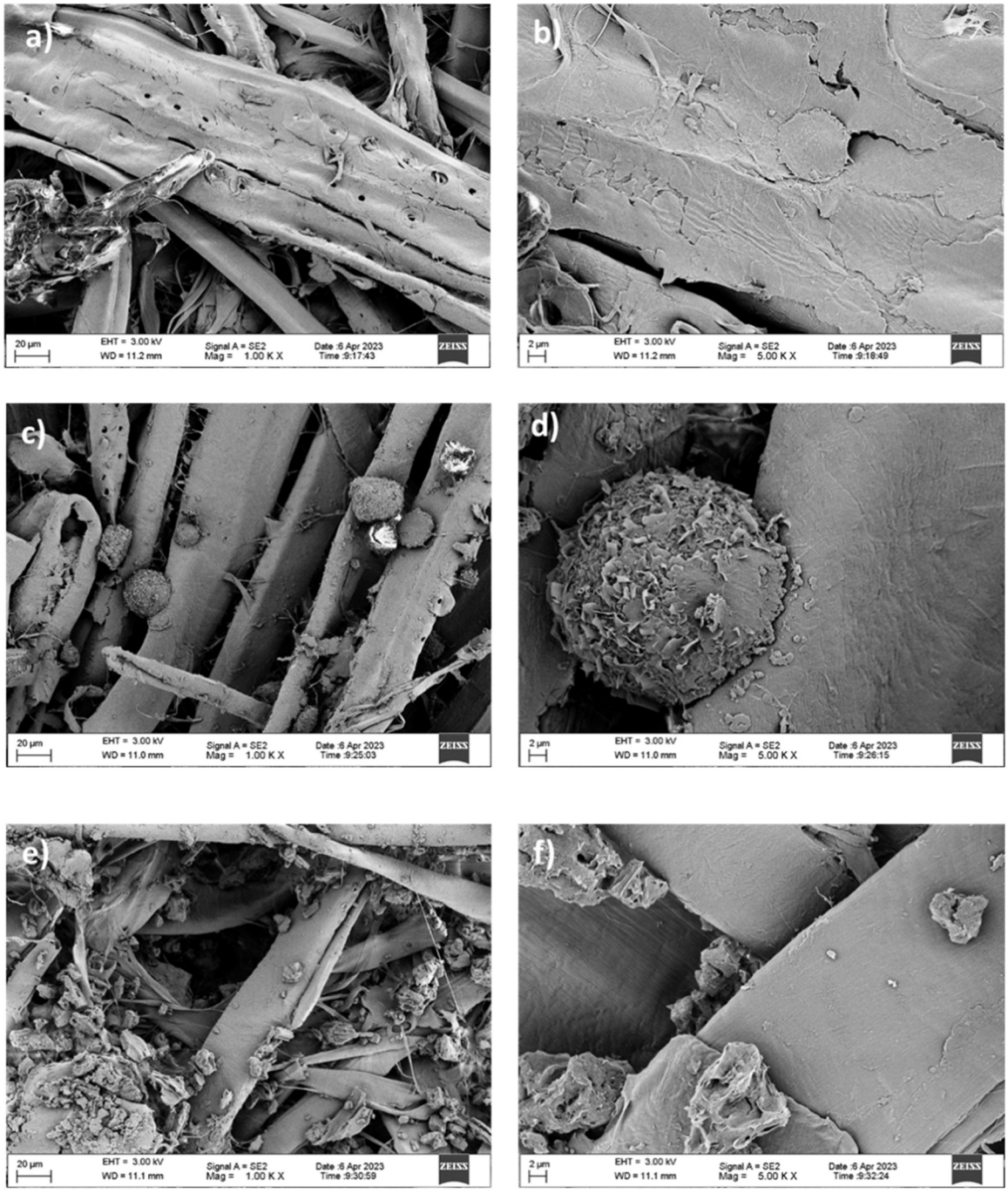

Fig. 4. SEM images of (a,b) TMP, (c,d) TMP AKD5 and (e,f) TMP MgSt5 at a magnification of 1000X (a,c,e) and 5000X (b,d,f).

the SEM images of the TMP-AKD sheets (Figs. 4b and 4c). Similarly, particles are visible in the SEM images of the TMP-MgSt sheets, as shown in Figs. 4d and 4e, albeit with less defined shape compared to the AKD. SEM images were also taken of sheets of TMP, TMP-AKD and TMP-MgSt, which had been exposed to heat of 100 and 180 °C. The images showed no visible AKD particles for any of the sheets exposed to 100 and 180 °C (Fig. S2). In case of MgSt addition, particles were still visible in the sheet exposed to 100 but no particles were observed after the sheet had been exposed to 180 °C (Fig. S2). The disappearance of visible particles at 100 °C for AKD and 180 °C for MgSt correspond to their different melting temperatures determined using DSC for the two additives, 62 and 130 °C, respectively (Fig. S3).

3.3. Friction between TMP and metal is reduced with increasing temperature

The average COF values for metal and TMP, metal and TMP AKD as well as metal and TMP MgSt samples were determined at 30, 100 and 180 °C and at a sliding speed of 50 mm/s. Fig. 5 illustrates a representative measurement of COF versus time for TMP-metal at 30 °C. The figure shows repetition of three different measurements yielding 50 data points each. The average COF used in comparison of the TMP sheets with added AKD and MgSt at different temperatures was calculated based on the three different repetitions. No trend towards reduced or increased COF over time is observed. The figure further shows the variations of measured COF obtained within one single run.

The COF of TMP and metal is statistically the same independent of

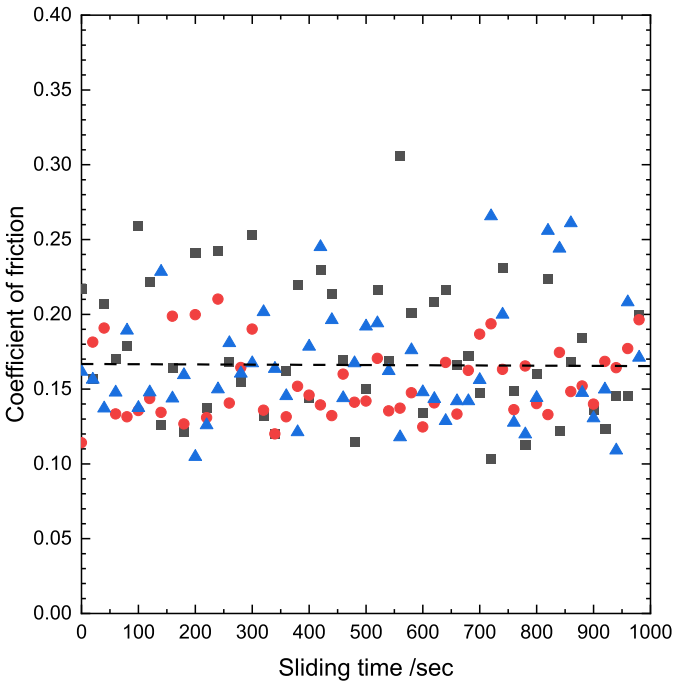

Fig. 5. Coefficient of friction vs time for TMP-metal at T = 30 °C at a speed of 50 mm/s and 30 °C where black squares, red circles and blue triangles depict three different measurements, resulting in the calculated average COF being 0.165 (dashed line) and standard deviation of 0.039.

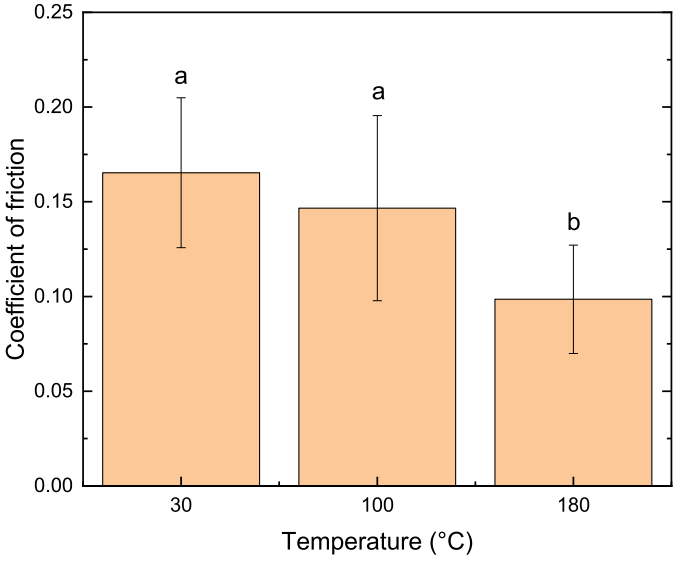

Fig. 6. Coefficient of friction of TMP sheets and metal as a function of temperature. Different small letters in each column show a statistically significant difference ($p < 0.05$).

temperature of 30 or 100 °C, but COF of TMP and metal is reduced at 180 °C (Fig. 6). Friction between wood and metal is known to reduce between 100 and 130 °C [21,22,27] and thereafter shown to increase again. The temperature at which the minimum COF is observed and exact temperature at which COF increases, differ between studies but trends are similar [21,22]. Svensson and co-workers explain the reduction in COF at temperatures between 100 and 120 °C to the presence of lubricating layer from naturally present fatty acids [27]. At higher temperature, the wood softens, and wear debris are observed [27]. Svensson and co-workers [27] explain the higher COF between

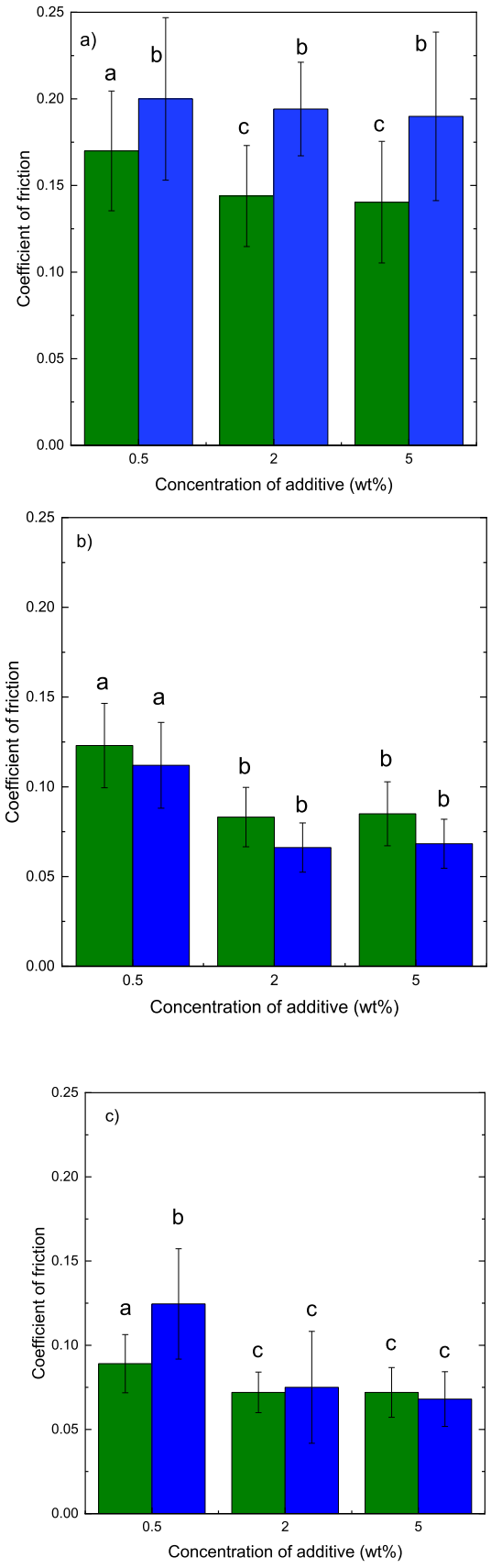

Fig. 7. COF of TMP and metal as a function of 0.5, 2 and 5 wt% addition of AKD (green) and MgSt (blue) at a) 30 °C, b) 100 °C and c) 180 °C. Different small letters in each column show a statistically significant difference ($p < 0.05$).

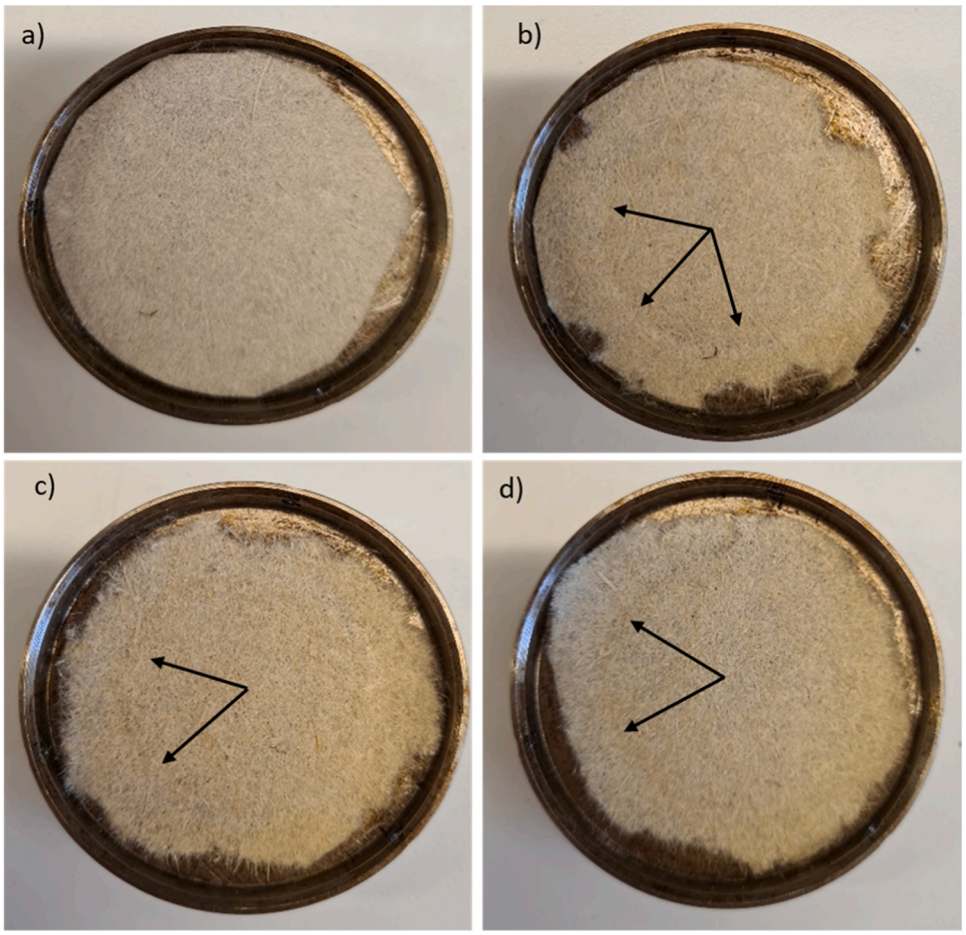

Fig. 8. Wear tracks indicated by arrow at a) TMP at T = 30 °C, b) TMP at T = 180 °C, c) TMP MgSt5 at 180 °C and d) TMP AKD5 at 180 °C. All images were taken after running distance of 50 m, a sliding speed of 100 mm/s and at an axial force of 1 N.

wood and metal at the higher temperatures as being related to the wear debris, as well as the softened wood structure, the latter is also the explanation by Murase 1979 [21], leading to increased surface contact and thus higher COF. The COF between TMP and metal does not seem to follow similar trend as wood and metal. Instead of an increase in COF between TMP and metal at 180 °C, we observe a reduction. Reduction of moisture content reduced COF between wood and metal [28], however, the thermogravimetric analysis, TGA, (Fig. S4) data reveals a weight difference of 2.8% between temperatures of 30 and 100 °C, and a smaller weight difference of 0.5% between temperatures of 100 and 180 °C for TMP. The largest step in moisture difference occurs thus between 30 and 100 °C, making the reduction in COF at 180 °C related to reduced moisture unlikely. The glass transition of lignin is 147 °C and lignin is reported to flow at 163 °C [29]. It is thus possible that changes in the physical behavior of lignin influences the reduction in COF of TMP and metal at 180 °C, especially, as lignin is exposed to a larger degree on TMP fibres compared to wood. However, the exact cause for COF reduction between metal and TMP will need to be further studied.

Fig. 7 shows the effect of increasing amounts of AKD and MgSt on COF between metal and TMP at different temperatures. At 30 °C, the smallest addition of AKD (0.5 wt%) did not change the COF between TMP and metal. Addition of AKD to a concentration of approx. 2 and 5 wt% reduced the friction between metal and TMP, however not in a linear fashion as the two concentrations reduced the COF between metal and TMP equally. Surprisingly, the addition of MgSt increased the COF between metal and TMP for all concentrations tested at 30 °C.

At 100 °C, addition of the AKD and MgSt reduced the COF between metal and TMP at any concentration, where the higher concentrations of 2 and 5 wt% of additive were most effective. AKD reduces the COF between TMP and metal to a larger degree than MgSt at 0.5 wt%, but the two additives are equally effective at the higher concentrations.

At 180 °C, COF between TMP and metal was not reduced at addition of 0.5 wt% AKD and increased using MgSt. At 2 and 5 wt% added AKD and MgSt, the COF reduced to an equal amount independent of additive.

The results presented in Fig. 7 show that elevated temperatures reduce the friction between metal and TMP. We speculate the reason could be softening of lignin, which then acts as a lubricant. Addition of AKD reduces the friction between TMP and metal for all studied temperatures, when added at 2 or 5 wt%. An addition of 0.5 wt%, AKD reduces COF between TMP and metal at 100 and 180 °C. The addition of MgSt shows only a reduction in COF between TMP and metal at the higher temperatures studied, and at higher concentrations (2 and 5 wt %). The additives (AKD or MgSt) were equally effective in reducing COF at 100 and 180 °C. In addition, we showed that increasing the addition of AKD or MgSt from 2 to 5 wt% has no benefit in terms of COF reduction. No correlation between the reduction in COF and melting temperature of the AKD or MgSt was observed given the melting of AKD occurs at 62 °C and of MgSt at 130 °C (Fig. S3). A potential increase in TMP surface temperature owing to friction was verified, and amounted to only 2 °C, why friction heat is not enough to have melted AKD or MgSt at the lower temperatures studied.

No visual tracks or damage were observed on the steel balls under the conditions used (Fig. S5). No visual wear track was observed on the TMP sheet itself at 30 °C (Fig. 8a). At 180 °C, the sheet was observed to go slightly brown and a track from the balls was observed, independent of additive or not (Fig. 8c-d).

Our results show that AKD functions as a lubricant between TMP and metal at broader range of temperature and at lower concentrations than MgSt. Indeed, addition of long chain AKD to paper has been shown to reduce paper-paper friction, where the mechanism is believed to be related to hydrocarbon chain orientation in sliding direction, and the ability of AKD to cover the fiber surface [29]. AKD and MgSt are equally effective as lubricants at temperatures relevant for extrusion (180 °C) and at concentrations of 2 - 5 wt%.

4. Conclusion

The COF between metal and TMP is reduced when the TMP and metal is exposed to high temperature (180 °C) compared to low temperature (30 °C). The addition of AKD reduces the COF for any temperature studied, if added at 2 – 5 wt%. MgSt reduces the COF between metal and TMP at 100 °C or above. Both additives (AKD and MgSt) are equally effective in reducing COF at temperatures > 100 °C. No linear reduction in COF between metal and TMP was observed upon increased additive concentration, instead the COF levels out at additions above 2 wt%. The addition of AKD and MgSt left the surface roughness of the TMP sheets unaltered at the normal force and concentrations studied. The study shows that AKD can be used for friction control of TMP-metal systems, but is visibly not contributing to reduced wear of TMP surface. Future studies will show if addition of AKD or MgSt can reduce surface defects from extruded plastic wood composites containing TMP, thus correlating friction to process parameters.

Statement of originality

This is to certify that the work and results in the manuscript named: Reducing friction between metal and thermos-mechanical pulp using alkyl ketene dimers and magnesium stearate written by Seyedehsan Hosseini, Roujin Ghaffari, Anette Larsson, Gunnar Westman and Anna Ström are solely performed by the authors. The text nor the results are plagiarism.

The study in itself, studying the effect of addition of alkyl ketene dimer and magnesium stearate on friction between metal and thermos-mechanical pulp, as a function of temperature, has as far as we are aware never been studied.

In general, friction studies of thermos-mechanical pulp is scarce or none existing, while studies on wood and metal exist.

CRediT authorship contribution statement

Larsson Anette: Conceptualization, Supervision, Writing – review & editing. **Westman Gunnar:** Funding acquisition, Writing – review & editing. **Ström Anna:** Conceptualization, Supervision, Writing – review & editing. **Hosseini Seyedehsan:** Investigation, Validation, Writing – original draft. **Ghaffari Roujin:** Investigation.

Declaration of Competing Interest

The authors declare that they have no known competing financial interests or personal relationships that could have appeared to influence the work reported in this paper.

Data Availability

Data will be made available on request.

Appendix A. Supporting information

Supplementary data associated with this article can be found in the online version at doi:10.1016/j.triboint.2024.109280.

References

[1] Brooks AL, Wang S, Jambeck JR. The Chinese import ban and its impact on global plastic waste. Sci Adv 2018;4:1–7. https://doi.org/10.1126/sciadv.aat0131.

[2] "Circular Economy: new rules on single-use plastics," accessed at: ⟨https://ec.europa.eu/commission/presscorner/detail/de/STATEMENT_19_1873⟩, 2019.

[3] Ashby MF, Cebon D. Materials selection in mechanical design. J Phys IV Fr 1993;03 (C7). https://doi.org/10.1051/jp4:1993701.

[4] Schirp A, Stender J. Properties of extruded wood-plastic composites based on refiner wood fibres (TMP fibres) and hemp fibres. Eur J Wood Prod 2010;68: 219–31. https://doi.org/10.1007/s00107-009-0372-7.

[5] Akpan EI, Wetzel B, Friedrich K. A fully biobased tribology material based on acrylic resin and short wood fibres. Tribol Int 2018;120:381–90. https://doi.org/10.1016/j.triboint.2018.01.010.

[6] Hristov V, Takács E, Vlachopoulos J. Surface tearing and wall slip phenomena in extrusion of highly filled HDPE/wood flour composites. Polym Eng Sci 2006;46: 1204–14. https://doi.org/10.1002/pen.20592.

[7] George J, Janardhan R, Anand JS, Bhagawan SS, Thomas S. Melt rheological behaviour of short pineapple fiber reinforced low density polyethylene composites. Polymer 1996;37:5421–31. https://doi.org/10.1016/S0032-3861(96)00386-2.

[8] Mazzanti V, Mollica F. A review of wood polymer composites rheology and its implications for processing. Polymers 2020;12:2304–27. https://doi.org/10.3390/polym12102304.

[9] Pashazadeh S, Ghanbari R, Bek M, Aulova A, Moberg T, Brolin A, Kádár R. Mapping surface defects in highly-filled wood fiber polymer composite extrusion from inline spectral analysis. Compos Sci Technol 2023;242:110133. https://doi.org/10.1016/j.compscitech.2023.110133.

[10] Wang Y, Jia Z, Ji J, Wei B, Heng Y, Liu D. Wear behaviour and microstructure evolution in pure nickel extrusion manufacturing. T Nonferr Met Soc 2023;33: 1472–91. https://doi.org/10.1016/S1003-6326(23)66197-7.

[11] Hosseini S, Nilsson R, Ström A, Larsson A, Westman G. Alkyl ketene dimer modification of thermomechanical pulp promotes processability with polypropylene. Polym Compos 2023:1–11. https://doi.org/10.1002/pc.27818.

[12] Karademir A, Hoyland D, Wiseman N, Xiao H. A study of the effects of alkyl ketene dimer and ketone on paper sizing and friction properties. Appita J 2004;57:116–20.

[13] Lindstrom T, O'Brian H. On the mechanism of sizing with alkylketene dimers: Part 2. The kinetics of reaction between alkylketene dimers and cellulose. NPPRJ 1986; 1:34–42. https://doi.org/10.3183/npprj-1986-01-01-p034-042.

[14] Leinonen UI, Jalonen HU, Vihervaara PA, Laine ES. Physical and lubrication properties of magnesium stearate. J Pharm Sci 1992;81:1194–8. https://doi.org/10.1002/jps.2600811214.

[15] Wada Y, Matsubara T. Pseudopolymorphism and lubricating properties of magnesium stearate. Powder Technol 1994;78:109–14. https://doi.org/10.1016/0032-5910(93)02782-6.

[16] Chin WC, Yousif BF. Potential of kenaf fibres as reinforcement for tribological applications. Wear 2009;267:1550–7. https://doi.org/10.1016/J.WEAR.2009.06.002.

[17] Yallew TB, Kumar P, Singh I. Sliding wear properties of jute fabric reinforced polypropylene composites. Procedia Eng 2014;97:402–11. https://doi.org/10.1016/J.PROENG.2014.12.264.

[18] Behera S, Gautam RK, Mohan S, Chattopadhyay A. Hemp fiber surface modification: its effect on mechanical and tribological properties of hemp fiber reinforced epoxy composites. Polym Compos 2021;42:5223. https://doi.org/10.1002/pc.26217.

[19] Guan N, Thunell B, Lyth K. On the friction between steel and some common swedish wood species. Holz als Roh-und Werkst 1983;41:55–60. https://doi.org/10.1007/BF02612232.

[20] Murase Y. Effect of temperature on friction between wood and steel. J Jpn wood Res Soc 1979;25:264–72.

[21] Engberg BA, Rundlöf M, Höglund H. Sliding friction between wood and steel in a saturated steam environment. J Pulp Pap 2006;32:38–43.

[22] Yin W, Lu H, Zheng Y, Tian Y. Tribological properties of the rotary friction welding of wood. Tribol Int 2022;167:107396.

[23] Wan S, Tieu AK, Xia Y, Zhu H, Tran HB, Cui S. An overview of inorganic polymer as potential lubricant additive for high temperature tribology. Tribol Int 2016;102: 620–35. https://doi.org/10.1016/j.triboint.2016.06.010.

[24] Hosseini S, Venkatesh A, Boldizar A, Westman G. Molybdenum disulphide - a traditional external lubricant that shows interesting interphase properties in pulp-based composites. Polym Compos 2021;42:4884–96. https://doi.org/10.1002/pc.26197.

[25] Kangas H, Kleen M. Surface chemical and morphological properties of mechanical pulp fines. NPPRJ 2004;19:191–9. https://doi.org/10.3183/npprj-2004-19-02-p191-199.

[26] Forming handsheets for physical tests of pulp, test method TAPPI/ANSI T 205 sp-18, 2006.

[27] Svensson BA, Nyström S, Gradin PA, Höglund H. Frictional testing of wood-Initial studies with a new device. Tribol Int 2009;42:190–6. https://doi.org/10.1016/j.triboint.2008.03.009.

[28] Murase Y. Frictional Properties of Wood at High Sliding Speed. J Jpn wood Res Soc 1980;26:61–5.

[29] (a) Akato KM, Nguyen NA, Rajan K, Harper DP, Naskar AK. A tough and sustainable fiber-forming material from lignin and waste poly(ethylene terephthalate). RSC Adv 2019;9:31202–11. https://doi.org/10.1039/c9ra07052d. (b) Karademir A, Hoyland DV, Wiseman N, Xiao H. A study of the effects of alkyl ketene dimer and ketone on paper sizing and friction properties. Appita J 2004;57: 116–20.